

# Model-Informed Precision Dosing of Isoniazid: Parametric Population Pharmacokinetics Model Repository

Gehang Ju<sup>1-3</sup>, Xin Liu<sup>1-3</sup>, Wenyu Yang<sup>4</sup>, Nuo Xu<sup>4</sup>, Lulu Chen<sup>3,5</sup>, Chenchen Zhang<sup>6</sup>, Qingfeng He<sup>4</sup>, Xiao Zhu<sup>4,\*</sup>, Dongsheng Ouyang<sup>1-3,5,\*</sup>

<sup>1</sup>Department of Clinical Pharmacology, Xiangya Hospital, Central South University, Changsha, People's Republic of China; <sup>2</sup>Institute of Clinical Pharmacology, Central South University, Changsha, People's Republic of China; <sup>3</sup>Hunan Key Laboratory for Bioanalysis of Complex Matrix Samples, Changsha Duxact Biotech Co., Ltd, Changsha, People's Republic of China; <sup>4</sup>Department of Clinical Pharmacy, School of Pharmacy, Fudan University, Shanghai, People's Republic of China; <sup>5</sup>Changsha Duxact Biotech Co., Ltd, Changsha, People's Republic of China; <sup>6</sup>School of Pharmaceutical Sciences, Sun Yat-sen University, Guangzhou, People's Republic of China

\*These authors contributed equally to this work

Correspondence: Dongsheng Ouyang; Xiao Zhu, Email 801940@csu.edu.cn; xiaozhu@fudan.edu.cn

**Introduction:** Isoniazid (INH) is a crucial first-line anti tuberculosis (TB) drug used in adults and children. However, various factors can alter its pharmacokinetics (PK). This article aims to establish a population pharmacokinetic (popPK) models repository of INH to facilitate clinical use.

**Methods:** A literature search was conducted until August 23, 2022, using PubMed, Embase, and Web of Science databases. We excluded published popPK studies that did not provide full model parameters or used a non-parametric method. Monte Carlo simulation works was based on RxODE. The popPK models repository was established using R. Non-compartment analysis was based on IQnca.

**Results:** Fourteen studies included in the repository, with eleven studies conducted in adults, three studies in children, one in pregnant women. Two-compartment with allometric scaling models were commonly used as structural models. NAT2 acetylator phenotype significantly affecting the apparent clearance (CL). Moreover, postmenstrual age (PMA) influenced the CL in pediatric patients. Monte Carlo simulation results showed that the geometric mean ratio (95% Confidence Interval, CI) of PK parameters in most studies were within the acceptable range (50.00–200.00%), pregnant patients showed a lower exposure. After a standard treatment strategy, there was a notable exposure reduction in the patients with the NAT2 RA or nonSA (IA/RA) phenotype, resulting in a 59.5% decrease in AUC<sub>0-24</sub> and 83.2% decrease in C<sub>max</sub> (Infants), and a 49.3% reduction in AUC<sub>0-24</sub> and 73.5% reduction in C<sub>max</sub> (Adults).

**Discussion:** Body weight and NAT2 acetylator phenotype are the most significant factors affecting the exposure of INH. PMA is a crucial factor in the pediatric population. Clinicians should consider these factors when implementing model-informed precision dosing of INH. The popPK model repository for INH will aid in optimizing treatment and enhancing patient outcomes.

**Keywords:** Isoniazid, model-informed precision dosing, population pharmacokinetics, nonlinear mixed-effects model

## Introduction

Globally, tuberculosis is a highly contagious disease that causes significant morbidity and mortality. It was the leading cause of death from a single infectious agent before the coronavirus (COVID-19) pandemic, surpassing even HIV/AIDS. According to the World Health Organization (WHO) tuberculosis report of 2022, 6.4 million people were newly diagnosed with TB. Although there was an 86% success rate for treating drug-susceptible TB in 2021,<sup>1</sup> a significant proportion of patients showed inadequate treatment response, primarily due to insufficient anti-TB drug exposure.<sup>2</sup>

In the field of TB management, isoniazid is considered the most crucial first-line drug for both adults and children.<sup>3</sup> The WHO recommends daily doses of 300mg (range, 4–5mg/kg) for patients aged 10 years and older, and 10mg/kg

(range, 7–15mg/kg) for those under 10 years, while also advising using body weight as a covariate to customize anti-TB administration.<sup>4</sup> The treatment outcome for first-line TB drugs is mainly predicted by the area under the concentration-time curve over a dosing interval ( $AUC_{0-24}$ ) relative to the minimal inhibitory concentration and peak concentration ( $C_{max}$ ).<sup>5–7</sup> For isoniazid, the desired exposure is  $C_{max}$  (3–6mg/L) and  $AUC_{0-24}$  (52mg\*h/L).<sup>7–9</sup>

Isoniazid is primarily metabolized by hepatic N-acetyltransferase 2 (NAT2) and is the main candidate among TB drugs for genotype-based dose individualization.<sup>10</sup> NAT2 phenotypes, such as slow acetylators (SA), intermediate acetylators (IA), and rapid acetylators (RA), have a significant impact on isoniazid clearance. Researchers have discovered that the probability of achieving an INH exposure associated with 90% of maximal early bactericidal activity (EBA) was 100% in SA and 96.3% in IA, but only 25% in RA after a standard dose of 5mg/kg.<sup>11</sup> Additionally, drug exposure can be influenced by several other factors, including poor adherence, malabsorption, intraindividual differences in pharmacokinetics, food intake, and HIV status.<sup>12–14</sup> Several studies have shown that current TB treatment regimens, which use a one-size-fits-all approach, may result in therapeutic failure and serious adverse reactions (ADRs), indicating a need for more precise methods to guide individual therapy.<sup>15–17</sup>

The use of model-informed precision dosing (MIPD) is an emerging approach for personalized drug therapy, with promising results.<sup>18</sup> The popPK approach, based on a nonlinear mixed-effects model, is a powerful tool for achieving this goal. PopPK can identify potential sources of variability and define the pharmacokinetic characteristics of a population. Monte-Carlo simulations can predict the effect of different factors on drug exposure and estimate the probabilities of achieving the desired treatment outcome. Previous studies have successfully applied this approach to other drugs and created model repositories,<sup>19–22</sup> which enable the use of model averaging/selection methods and enhance the prediction performance of MIPD.<sup>23,24</sup>

There have been systematic reviews on the pharmacokinetic models of isoniazid,<sup>25–27</sup> but two of these studies only provided descriptive introductions to existing articles.<sup>25,26</sup> Another study failed to quantitatively compare exposure differences among different models for the same virtual population after standard treatment and did not provide corresponding code files to assist other researchers in model replication.<sup>27</sup> Due to the complexity of models, data quality, and replication challenges, not all models could be replicated and included in the model repository. We further explored whether changes in covariate information, commonly discussed in existing models, have clinically significant implications. Additionally, we investigated the popPK model analysis in pregnant women, comparing whether pregnancy status results in differences in adult exposure. By establishing a model repository, researchers can modify population covariate features and administration strategies to compare patient exposures predicted by specific or different models, enabling the selection of the most clinically relevant model to enhance the accuracy of Model-Informed Precision Dosing (MIPD). Simultaneously, other model-based studies can benefit from the strengthened application value derived from the model repository.

## Methods

### Search Strategy

This article focused on the popPK model of isoniazid. Literature screening referred to the systematic review and meta-analysis search process. We screened PubMed, Web of Science and Embase database from its inception to 23 August 2022. The search terms included MeSH terms plus Entry terms, used: (“isoniazid” OR “tubazide” OR “isonex”) AND (“population pharmacokinetic” OR “pharmacokinetic model” OR “NONMEM” OR “nonlinear mixed effects model” OR “WINNONMIX” OR “NLME”) AND (“Tuberculosis” OR “Kochs Disease”). The literature search strategy is based on the Preferred Reporting Items for Systematic Reviews and Meta-analyses (PRISMA) reporting guideline. Two authors (Gehang Ju and Xin Liu) conducted the paper screening work independently and back-to-back, a third senior (Xiao Zhu) investigator was consulted to resolve any discrepancies. The paper management software was EndNote (Version 20; Thomson Scientific, Box Hill, Victoria, Australia).

The eligible popPK article should meet the following inclusion criteria: (1) study population: human (majority is TB patients); (2) dose regimen: oral; (3) modelling approach: a parametric nonlinear mixed-effects model; (4) languages:

only published in English. We excluded if (1) type of paper: reviews or methodology articles; (2) duplicated work; (3) missing important PK parameters or (4) model established with nonparametric methods.

## Data Extraction

Two authors independently extracted the following information from eligible articles: (1) baseline data: demographic data and laboratory test data (eg country, age, body weight, sex, NAT2 phenotype, etc.); (2) study characteristics: treatment regimens, sample number, bioanalytical methods, the lower limit of quantification, etc.; (3) popPK characteristics: model parameters and formula, structural models, covariates, covariates involved method, inter-individual variability, inter-occasion variability (IOV), and residual unexplained variability (RUV).

## Literature Quality Assessment

The assessment of the quality of the included studies was performed by utilizing a 33-item checklist, consisting of 5 categories, as presented in [Table S1](#), according to previous popPK systematic review quality assessment method.<sup>19–22</sup> This checklist was designed to assess the essential components required for the reporting of clinical pharmacokinetic (PK) studies. For each item, one point was assigned if the involved literature met the criteria, whereas incomplete data were assigned 0.5 points. If the item did not meet the criteria, it was assigned 0 points. To evaluate the quality of each population pharmacokinetic (popPK) study, compliance was calculated using the following equation:

$$\text{Compliance (\%)} = (\text{sum of items reported} / \text{sum of all items}) * 100\%$$

## Comparison of the Retrieved Study

The study analyzed the impact of identified covariates on CL and other critical pharmacokinetic parameters. To facilitate comparison, continuous covariates were standardized to the same range, whereas binary covariates, such as HIV status, were coded as 0 for negative and 1 for positive. The minimum and maximum CL values were determined based on the range of covariates identified in each study. The median covariate values were normalized to the reference value of CL, and the effect of covariates on CL was expressed as a percentage of the CL range divided by the CL reference value for each study. Forest mapping was employed to summarize and compare the identified covariates' impact on CL. The percentage range of the effect of identified covariates on CL was computed using the formula:

$$\text{Covariate effect} = \frac{\text{The minimum/maximum CL}}{\text{Reference CL}} * 100\%$$

A change in CL within the 80% to 125% range was considered to have no clinical significance according to bioequivalence standards.<sup>19–21</sup>

## Application of the popPK Model Repository

### Monte Carlo Simulation

To assess the statistical and structural models of the popPK studies, Monte Carlo simulations of concentration-time profiles were performed, which also provided visual predictive distributions (VPDs). It was assumed that the published models were sufficient to describe the data, and a predictive distribution of the simulated isoniazid concentration for each model would fully represent the original data and its significant features. The RxODE package (version 1.1.5, <https://CRAN.R-project.org/package=RxODE>) was utilized for solving and simulating ODE-based models. One thousand virtual patients were simulated for each identified study, and the concentration-time profiles were plotted according to the popPK model using R software (version 4.2.2).

The VPDs incorporated the effects of body weight (BW)/Fat-free Mass (FFM), postmenstrual age, and NAT2 phenotype. Virtual patients were defined as either infants (14 kg, 2 years, NAT2 SA/IA/RA) or adults (60 kg/46 kg, NAT2 SA/IA/RA). Oral administration of 300 mg QD for adults and 150 mg QD for infants, based on existing treatment standards,<sup>4</sup> was determined to be the administration strategy. All patients were assumed to receive multi-doses of isoniazid to reach the steady state.

## Simulation Comparison

In this study, the non-compartment analysis (NCA) of plasma concentrations of virtual patients in different models was performed to analyze and compare isoniazid exposure in the typical population after standard treatment. Monte Carlo simulation was used to generate the NCA results for each model. To ensure the comparability of simulation results, only the slow acetylators of NAT2 were selected for NCA. Upper and lower limits of 95% confidence intervals (CI) and the geometric mean were calculated for  $C_{\max}$ ,  $AUC_{0-24}$ . The geometric mean values of  $C_{\max, \text{geomean}}$  and  $AUC_{0-24, \text{geomean}}$  were also calculated for all virtual patients. To quantify the difference in typical population PK prediction for each model, the following equations were used:

$$C_{\max, \text{difference}} = (95\% \text{ CI of } C_{\max} / C_{\max, \text{geomean}}) * 100\%$$

$$AUC_{0-24, \text{difference}} = (95\% \text{ CI of } AUC_{0-24} / AUC_{0-24, \text{geomean}}) * 100\%$$

The geometric mean ratio and 95% CI of  $C_{\max}$  and  $AUC_{0-24}$  in the range of 50.00–200.00% were considered to indicate no difference in model prediction. The PK parameters, including  $C_{\max}$ ,  $AUC_{0-24}$  (log-linear trapezoidal rule), the peak time ( $T_{\max}$ ), and the half-life time ( $T_{1/2}$ ) were calculated using IQnca (Version 1.3.0, <https://iqnca.intiquan.com>) and Rmisc (Version 1.5.1, <https://www.rdocumentation.org/packages/Rmisc/versions/1.5.1>) package. All graphical displays, such as forest maps, were generated using R software (version 4.2.2).

## Results

### Study Identification

A total of 1699 studies were identified, comprising 472 articles from PubMed, 475 articles from Embase, 747 articles from Web of Science, and 4 articles from literature citations or other sources. Subsequently, a total of 14 articles were selected for the model repository. The flowchart illustrating the screening process for study identification can be found in [Figure S1](#).

[Figure 1](#) and [Table S1](#) display the quality results of the popPK studies. The median value for compliance with each included study was 93.5%, with a range of 86.4% to 97.0%. However, most studies failed to provide information on the methods used to handle missing data in the method section and the schematics of the final model in the results section. Notwithstanding, all the studies were of good overall quality, and there was no significant publication bias observed.<sup>13,28–40</sup>

### Literature Characteristics

#### Basic Characteristics

All the studies included in this analysis were published during 2011 to 2022. The majority of subjects across the studies were diagnosed with tuberculosis, with 3 studies specifically conducted on pediatric patients,<sup>29,30,32</sup> 11 studies on adult patients.<sup>13,28,31,33–40</sup> One of the adult studies was from pregnant women.<sup>35</sup> Among the 14 studies, 7 enrolled patients with both tuberculosis and HIV,<sup>13,28–30,36,38,40</sup> while only one study included both patients and healthy subjects.<sup>33</sup> The plasma isoniazid concentrations were determined using either liquid chromatography with ultraviolet detection or mass spectrometry, with the lowest limit of quantification ranging from 0.01 to 0.5 mg/L. Detailed characteristics of the included studies are provided in [Table 1](#).

#### Population Pharmacokinetic Characteristics

Twelve of the 14 popPK analyses were conducted using NONMEM (Icon, Dublin, Ireland),<sup>13,28,30–36,38–40</sup> two study based on Monolix (Lixoft, Antony, France).<sup>29,37</sup> The first-order conditional estimation with the  $\eta$ - $\epsilon$  interaction (FOCE-I) was the most commonly used algorithm. Most studies described the PK of isoniazid using a two-compartment model with first-order absorption and elimination. Only 4 studies used either internal or external evaluation. The visual predictive check (VPC), Bootstrap and goodness-of-fit (GOF) plot being the commonly used methods. The allometric growth model was used in all pediatric popPK models. The model characteristics and PK parameters of all studies were presented in [Table 2](#).

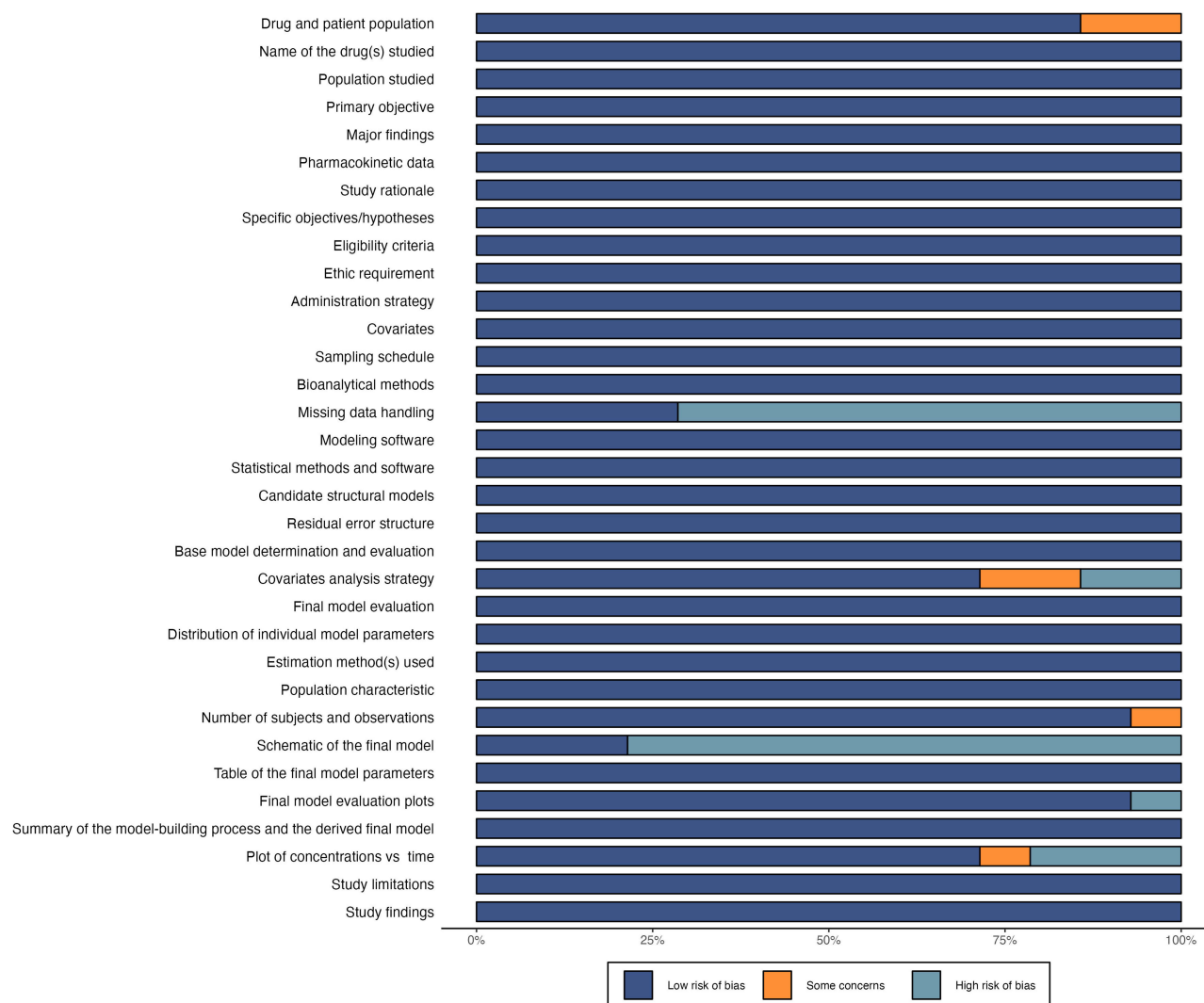


**Figure 1** Risk-of-bias assessments of isoniazid popPK studies.

IIV was described by an exponential model in all studies. The median coefficient of variation (CV) for IIV of CL was reported in five articles, volume of the central compartment ( $V_c$ ) in one article, intercompartmental clearance ( $Q$ ) in four articles, and volume of the peripheral compartment ( $V_p$ ) in three articles, with all exceeding 50%. Seven studies fixed more than three of the IIV for PK parameters to increase model stability. RUV was described by proportional models in three studies, additive models in four articles, exponential models in two studies, and combined proportional and additive models in five studies. All proportional RUV values were less than 50%, whereas additive RUV ranged from 0.0393 to 0.474, and exponential RUV ranged from 0.251 to 0.418, equivalent to proportional RUV ranging from 28.5% to 51.9%. Some studies reported the existence of IOV in  $K_a$ , bioavailability ( $F$ ), lag-time ( $T_{lag}$ ), and model transit time (MTT).

All models were evaluated internally, with diagnostic plots, bootstrap, and VPC being the most commonly used methods. Two studies employed the normalized prediction distribution error (NPDE).<sup>31,34</sup> Four studies were evaluated using an independent dataset, demonstrating acceptable predictability.<sup>33,34,37,39</sup> To improve the predictive performance of popPK models, external validation is recommended.

## Covariates of Inclusion

The majority of studies aimed to identify covariates that explain the IIV of isoniazid pharmacokinetics. A stepwise approach involving forward inclusion and backward elimination was commonly employed for covariate screening. A summary of all

**Table 1** Characteristics of Included Population Pharmacokinetic Studies

Study (Publication Year)	Type of Study	Country	Subjects	No. of Subjects (M/F)	Age(year) Mean±SD Median [Range]	Weight(Kg) Mean±SD Median [Range]	NAT2 Phenotype (RA / IA / SA)	No. of Observation	Sampling design	Dosage regimen Mean±SD	Bioassay [LOQ](mg/L)
Soedarsono S. (2022) <sup>28</sup>	Prospective	Indonesian	TB	107 (63/44)	43[18–77]	50[32–82]	16/49/42	153	0-24h Outpatients: 1 sample; Inpatients: 2 samples	100,150,200,225,250, 300,375,400,450, 600mg/d	HPLC-MS/MS [0.2]
Horita Y. (2018) <sup>29</sup>	Retrospective	Ghana	Children TB	113 (63/50)	5.00[2.17–8.25]	14.3[9.70–20.1]	12/50/51	561	0 h (predose) and 1, 2, 4, 8h (postdose)	11.0mg/kg/d	LC-MS/MS [0.1]
Denti P. (2022) <sup>30</sup>	Retrospective	Malawi South Africa	Children TB	180 (106/74)	2.03[0.219–11.9]	10.9[3.20–28.8]	26/81/35 Unknown: 38	843	0 h (predose) and 1, 2, 4, 6, 8h (postdose)	150 [3.75–300]mg/d	LC-MS/MS [0.1]
Jing W. (2020) <sup>31</sup>	Prospective	China	TB	89 (59/30)	44[16–72]	58[35–100]	32/38/19	195	Steady state 0.5–6h	300,600mg	LC-MS/MS [0.1]
Panjasawatwong N. (2020) <sup>32</sup>	Prospective	Vietnam	Children TB	100 (56/44)	3.0[0.167–15.0]	10.9[4.0–43]	17/47/28 Unknown: 8	523	A total of six plasma samples were collected on days 1, 14, 30, and 90. Two plasma samples were randomly drawn at 2 of 10 possible time points (ie, 1, 2, 3, 4, 5, 6, 8, 12, 18, or 24 h after dose) on each of days 1 and 14, and an additional plasma sample was randomly drawn at 3, 4, or 5 h postdose on each of days 30 and 90	5mg/kg/d	LC-MS/MS Plasma[0.012] CSF[0.036]
Chen B. (2022) <sup>33</sup>	Retrospective	China	Healthy and TB patient	Study1: 24 (24/0)  Study2: 21 (21/0)	Study1: 24.4±2.12  Study2: 24.1±2.61	Study1: 64.6±5.82  Study2: 63.0±5.82	Study1: 8/8/8  Study2: 11/9/1	NR	Study1: 0h (predose) and 0.25, 0.5, 1, 1.5, 2, 3, 4, 6, 8, 10, 14h (postdose); Study2: 0h (predose) and 0.25, 0.5, 1, 1.5, 2, 4, 6, 9, 12h (postdose); Study3: 2 and/or 6h (postdose)	Study1: 3*100mg Study2: 320mg once Study3: NA	HPLC [0.13]
Huerta-García AP. (2020) <sup>34</sup>	Prospective	Russia	Pulmonary or extra-pulmonary TB patient	157 (89/68) 69 (36/33)	42.2±11.5 45.5±16.4	56.5±9.7 57.1±14.1	72/62/23 13/32/24	385	Outpatients: 2, 4h (postdose); Inpatients: 0h (predose) and 0.33, 0.67, 1, 1.5, 2, 2.5, 3, 4, 6, 8, 12h (postdose)	≤50kg: 225mg QD; >50kg: 300mg QD	HPLC-UV [0.5]

Abdelwahab MT. (2020) <sup>35</sup>	Prospective	South Africa	TB pregnant patients	29	28.1 [25.2–29.9]	Prepartum: 66.0 [60.0–80.0]; Postpartum: 63.5 [57.3–72.8]	3/10/11 Unknown: 5	141	0h (predose) and 2, 4, 6, 8h (postdose)	Intensive phase: 75mg QD; Continuous phase: 75/150 mg QD	LC-MS/MS [0.195]
Wilkins JJ. (2011) <sup>13</sup>	Retrospective	South Africa	TB	Study1: 91 (67/24) Study2: 144 (66/78)	Study1: 37[23–60] Study2: 36[20–60]	Study1: 52.5[37.5–66.9] Study2: 46.1[31.2–68.0]	NR	2352	Study1: random times between 0–12h (postdose); Study2: 0h (predose) and 0.5, 1, 1.5, 2, 2.5, 3, 4, 6, 8h (postdose)	Study1: 100–400mg; Study2: 200–450mg/d	HPLC-UV [0.2]
McCallum A. D. (2021) <sup>36</sup>	Prospective	Malawian	TB	157 (120/37)	34 [28–39]	51.1 [46.9–55.6]	NR	750 (plasma and intrapulmonary)	Plasma: 1, 3h or 2, 4h postdose; Intrapulmonary: 0.5, 1, 3, 5h or 2, 4, 6, 8h postdose	Mean 4.7mg/kg	LC-MS/MS [0.02]
Gao Y. (2021) <sup>37</sup>	Prospective	China	TB	217 (147/41)	Group1: 40.1±11.1 Group2: 40.2±10.8 Group3: 40.4±11.2 Group4: 41.9±9.8 Validate: 40.8±11.1	Group1: 51.4±10.1 Group2: 51.9±9.4 Group3: 51.8±9.2 Group4: 53.4±10.1 Validate: 51.6±9.0	Group1: 21/16/10 Group2: 37/27/19 Group3: 20/9/10 Group4: 22/18/8 Validate: 28/24/9	1230	0 h (predose) and 1, 2, 4, 6, 8h (postdose)	<=50kg: 225 mg >50kg: 300 mg	LC-MS/MS [0.01]
Sundell J. (2020) <sup>38</sup>	Prospective	Rwanda	TB HIV	63 (37/26)	39.0[21.0–57.0]	49.0[30–68]	5/30/28	432	0h (predose) and 1, 2, 3, 4, 6, 8h (postdose)	150–300 mg	LC-MS/MS [0.08]
Cho Y. S. (2021) <sup>39</sup>	Prospective	South Korea	TB	454 (303/149)	55.4±17.4	60.0±11.7	184/212/53	477	0h (predose) and 0–24h (postdose)	100–400 mg	HPLC-MS/MS [0.1]
Naidoo A. (2019) <sup>40</sup>	Prospective	South Africa	TB HIV	58 (41/17)	37[31–42]	56.9[51.1–65.2]	18/43/34	573	0h (predose) and 2.5, 6, 24h (postdose)	225–300 mg	LC-MS/MS [0.02]

**Abbreviations:** HPLC, high-performance liquid; LC-MS/MS, liquid chromatograph mass spectrometer or mass spectrometer; LOQ, lower limits of quantification; NR, not reported; TB, tuberculosis; NAT2, N-acetyltransferase 2; SA, slow acetylators; IA, intermediate acetylators; RA, rapid acetylators.

**Table 2** Modelling Strategies and Final Pharmacokinetic Parameters of Included Studies

Study (Publication Year)	Software/Algorithm	Structural Model	Fixed Effect Parameters	Interindividual Variability	Residual Variability Prop: % Add: ng/mL	Internal Validation	External Validation (N=number of Samples)	Model Application
Soedarsono S. (2022) <sup>28</sup>	NONMEM (FOCE-I)	1 CMT with FO absorption and FO elimination	CL (L/h) = $17.7*(1+NAT2)*(BW/50)^{0.75}$ 0 for SA; 1.14 for IA; 2.16 for RA V (L) = $40.5*(BW/50)$ Ka (h <sup>-1</sup> ) = 0.25	82.5% – –	Add: 0.174	Bootstrap GOF VPC	NR	Dose recommendations based on C <sub>max</sub> and AUC <sub>0-24</sub>
Horita Y. (2018) <sup>29</sup>	Monolix (SAEM)	2 CMT with FO absorption and linear elimination	CL (L/h) = $NAT2*(BW/14.3)^{0.75}$ 4.44 for SA; 8.08 for others Vc (L) = $16.6*(BW/14.3)$ Q (L/h) = $8.46*(BW/14.3)^{0.75}$ Vp (L) = $1.07*(BW/14.3)$ Ka (h <sup>-1</sup> ) = 4.23	48% for RA/IA; 32.4% for SA 24.10% 63.70% 190% 56.70%	Prop: 19.3% Add: 0.0393	GOF VPC	NR	Probabilities of target attainment: AUC <sub>τ</sub> ≥ 11.95; C <sub>max</sub> ≥ 3/6
Denti P. (2022) <sup>30</sup>	NONMEM (FOCE-I)	2 CMT with FO absorption and elimination	CL (L/h) = $NAT2*PMA^{3.35}/(PMA^{3.35}+0.829^{3.35})$ $*(BW/9)^{0.75}$ 3.0 for SA; 4.65 for IA; 5.9 for RA Vc (L) = $10.5*(BW/9)$ Q (L/h) = $0.364*(BW/9)^{0.75}$ Vp (L) = $3.04*(BW/9)$ F = 1; when AGE > 2.72 0.74 + (1 - 0.74) * AGE / 1.63; when AGE < 2.72 Tlag (h) = 0.123 Ka (h <sup>-1</sup> ) = 2.83	30.80% – – – 31.1% (BOV) 132% (BOV) 48.7% (BOV)	Prop: 8.19% Add: 0.0610	Bootstrap GOF VPC	NR	Probabilities of target attainment: AUC
Jing W. (2020) <sup>31</sup>	NONMEM (FOCE-I)	2 CMT with oral absorption	CL (L/h) = $31.4*(BW/58)^{0.93}*NAT2$ 0.378 for SA; 1 for IA; 1.36 for RA Vc (L) = 21.1 Q (L/h) = 43.7 Vp (L) = 27.7 Ka (h <sup>-1</sup> ) = 1.70	50.60% – 79.87% – 87.06%	Expo: 0.251	Bootstrap GOF NPDE VPC	NR	Probabilities of target attainment: AUC <sub>0-24</sub> ≥ 10.52; C <sub>max</sub> ≥ 2.19/3/6
Panjasawatwong N. (2020) <sup>32</sup>	NONMEM (FOCE-I)	2 CMT disposition with 2 transit absorption CMT	CL (L/h) = $9.43*(BW/10.9)^{0.75}*(1-NAT2)$ $*MAT^{4.7}/(MAT^{4.7}+12.7^{4.7})$ 0.564 for SA; 0 for others F = 1 Vc (L) = $3.78*(BW/10.9)$ MTT (h) = 0.878 NT = 2 Ka (h <sup>-1</sup> ) = (NT+1)/MTT Q (L/h) = $28.0*(BW/10.9)^{0.75}$ Vp (L) = $15.3*(BW/10.9)$	36.80% – – – – – – – 101% –	Add: 0.474	GOF VPC	NR	Dose recommendations based on C <sub>max</sub> and AUC <sub>0-24</sub>

Chen B. (2022) <sup>33</sup>	NONMEM (FOCE-I)	1 CMT with FO absorption and FO elimination	CL (L/h) Vc (L) Ka (h-1)	$=28.7 \cdot e^{(-0.55 \cdot \text{NAT}2)}$ 2 for SA; 1 for IA; 0 for RA $=54.1$ $=3.91$	30.70% 19.40% 55.20%	$\sigma_{\text{LNH}}$ : Prop: 33.3% $\sigma_{\text{AclNH}}$ : Prop: 30.2%	Bootstrap GOF VPC	80	Probabilities of target attainment: fAUC/MIC $\geq$ 567
Huerta-García AP. (2020) <sup>34</sup>	NONMEM (FOCE-I)	2 CMT with FO absorption and elimination	CL (L/h) Vc (L) Q (L/h) Vp (L) Ka (h-1)	$=\text{NAT}2$ $=1.5 \cdot \text{BMI}$ $=9.9$ $=3.8$ $=2$	47.00% 59.40% – 114% 113.60%	Prop: 42.9%	Bootstrap GOF VPC NPDE	N=14	dose recommendations based on Cmaxations based on Cmax
Abdelwahab MT. (2020) <sup>35</sup>	NONMEM	2 CMT with 2 CMT disposition with FO elimination and transit CMT absorption	CL (L/h) Vc (L) Q (L/h) Vp (L) MTT (h) NN F	$=\text{NAT}2 \cdot (\text{BW}/65.3)^{0.75}$ 29.0 for SA; 75.7 for IA; 97.1 for RA $=130 \cdot (\text{BW}/65.3)$ $=12.4 \cdot (\text{BW}/65.3)^{0.75}$ $=28.5 \cdot (\text{BW}/65.3)$ $=1.21$ $=8.01$ $=1$	12.70% – – – 56.7% (BOV) – 36.7% (BOV)	Prop: 22.2% add: 0.045	VPC	NR	Dose recommendations based on Cmax and AUC <sub>0-24</sub>
Wilkins JJ. (2011) <sup>13</sup>	NONMEM (FOCE-I)	2 CMT with FO absorption and elimination and Tlag	CL (L/h) Vc (L) Q (L/h) Vp (L) Ka (h-1) Tlag (h) P <sub>last</sub> F	$=\text{NAT}2 \cdot (\text{BW}/70)^{0.75} \cdot (1 - 0.174 \cdot \text{HIV status})$ 9.7 for SA; 21.6 for others 1 for HIV positive; 0 for negative $=57.7 \cdot (\text{BW}/70) \cdot (1 - 0.103 \cdot \text{SEX})$ 0 for Males; 1 for Females $=3.34 \cdot (\text{BW}/70)^{0.75}$ $=1730 \cdot (\text{BW}/70)$ $=1.85$ $=0.18$ $=0.132$ $=1$	42.90% 40.62% 96.49% – 94.92% (BOV) 94.02% – 51.19% 28.98% (BOV)	Add: 0.205	Bootstrap VPC	NR	Probabilities of target attainment: AUC <sub>inf</sub> $\geq$ 10.52; C <sub>max</sub> $\geq$ 3-6
McCallum A. D. (2021) <sup>36</sup>	NONMEM (FOCE-I)	1 CMT with first-order absorption and first-order elimination	CL (L/h) V (L) Ka (h-1)	$=13.7$ $=78.5 \cdot (\text{BW}/51.1)^{1.08}$ $=3.29$	53.39% 23.87% –	expo: 0.418	GOF VPC	NR	Probabilities of target attainment: Cmax $\geq$ 3 ug/mL; Simulation AUC & C <sub>max</sub>

(Continued)

Table 2 (Continued).

Study (Publication Year)	Software/ Algorithm	Structural Model	Fixed Effect Parameters		Interindividual Variability	Residual Variability Prop: % Add: ng/mL	Internal Validation	External Validation (N=number of Samples)	Model Application
Gao Y. (2021) <sup>37</sup>	Monolix (FOCE)	2 CMT with FO absorption and elimination	CL (L/h)	= NAT2*(BW/50)^0.55	60.9%	Add: 0.178	GOF	61	Dose recommendations based on C <sub>max</sub> and AUC <sub>0-24</sub>
			NAT2	SA=12.6 IA=16.0 RA=30.6	-		VPC pcVPC		
			V <sub>c</sub> (L)	= 21.2	21.7%				
			Q (L/h)	= 8.7	-				
			V <sub>p</sub> (L)	= 125.8	-				
			K <sub>a</sub> (h <sup>-1</sup> )	= 0.68	23.6%				
Sundell J. (2020) <sup>38</sup>	NONMEM (FOCE-I)	2CMT with FO absorption with transit comp and FO elimination	CL (L/h)	= 9.2*NAT2*(BW/50)^0.75	82.7%	Prop: 34%	GOF	NA	Dose recommendations based on AUC <sub>0-24</sub>
			NAT2	SA = 1 IA = 1.32 RA = 2.29	-		VPC		
			V <sub>c</sub> (L)	= 41.3*(BW/50)	-				
			Q (L/h)	= 10.8*(BW/50)^0.75	120.6%				
			V <sub>p</sub> (L)	= 42.8*(BW/50)	-				
			MTT (h)	= 0.58	180.6%				
			NN	= 1 FIX	-				
			F (%)	= 100 FIX	27.2%				
Cho Y. S. (2021) <sup>39</sup>	NONMEM (FOCE-I)	2CMT with absorption lag time and sequential ZO (D0) and FO absorption with FO elimination	CL (L/h)	= 22.2*(1-NAT2)*(FFM/50)^0.75	14.0%	Prop:29.2% add: 0.134	GOF	91	Dose recommendations based on C <sub>max</sub> and AUC <sub>0-24</sub>
			NAT2	SA = 0.646 IA = 0.274 RA = 0	-		pcVPC Bootstrap		
			V <sub>c</sub> (L)	= 16.5*(FFM/50)	3.0% FIX				
			Q (L/h)	= 18.4	-				
			V <sub>p</sub> (L)	= 36.4	15.0% FIX				
			K <sub>a</sub> (h <sup>-1</sup> )	= 1.21	60.0% FIX				
			Tlag (h)	= 0.02 FIX	22.0% FIX				
			D0 (h)	= 0.47	20.0% FIX				
Naidoo A. (2019) <sup>40</sup>	NONMEM (FOCE-I)	2CMT with FO absorption and elimination	CL (L/h)	= NAT2*(FFM/47)^0.75	13.0% (BOV)	Prop: 19.3% add: 0.0393	VPC	NA	NA
			NAT2	SA = 17.4 IA = 28.4 RA = 40.5	-		Bootstrap		
			V <sub>c</sub> (L)	= 73.4*(FFM/47)	26.3%				
			Q (L/h)	= 1.1*(FFM/47)^0.75	-				
			V <sub>p</sub> (L)	= 19.8*(FFM/47)	-				
			K <sub>a</sub> (h <sup>-1</sup> )	= 0.13	23.5% (BOV)				
			F (%)	= 100 FIX	27.4% (BOV)				

**Abbreviations:** CL, apparent clearance (L/h); Q, the intercompartment clearance; V, apparent volume of distribution (L); V<sub>c</sub>, the apparent central compartment distribution volumes (L); V<sub>p</sub>, the apparent peripheral compartment distribution volumes (L); K<sub>a</sub>, absorption rate (h<sup>-1</sup>); F, bioavailability; Tlag, lag time (h); MTT, mean transit absorption time; NT, transit absorption compartment; Pfast: Proportion of fast eliminators in population; FOCE, first order conditional estimation; FOCE-I, FOCE with the interaction; SAEM, stochastic approximation expectation maximization; GOF, goodness-of-fit plot; VPC, visual predictive check; NPDE, normalized prediction distribution errors; NAT2, N-acetyltransferase 2; SA, slow acetylators; IA, intermediate acetylators; RA, rapid acetylators; BW, body weight; BMI, body mass index; PMA, postmenstrual age; FFM, Fat-free Mass; C<sub>max</sub>, peak plasma concentration (mg/L); AUC, area under the plasma concentration-time curve; NR, not reported.

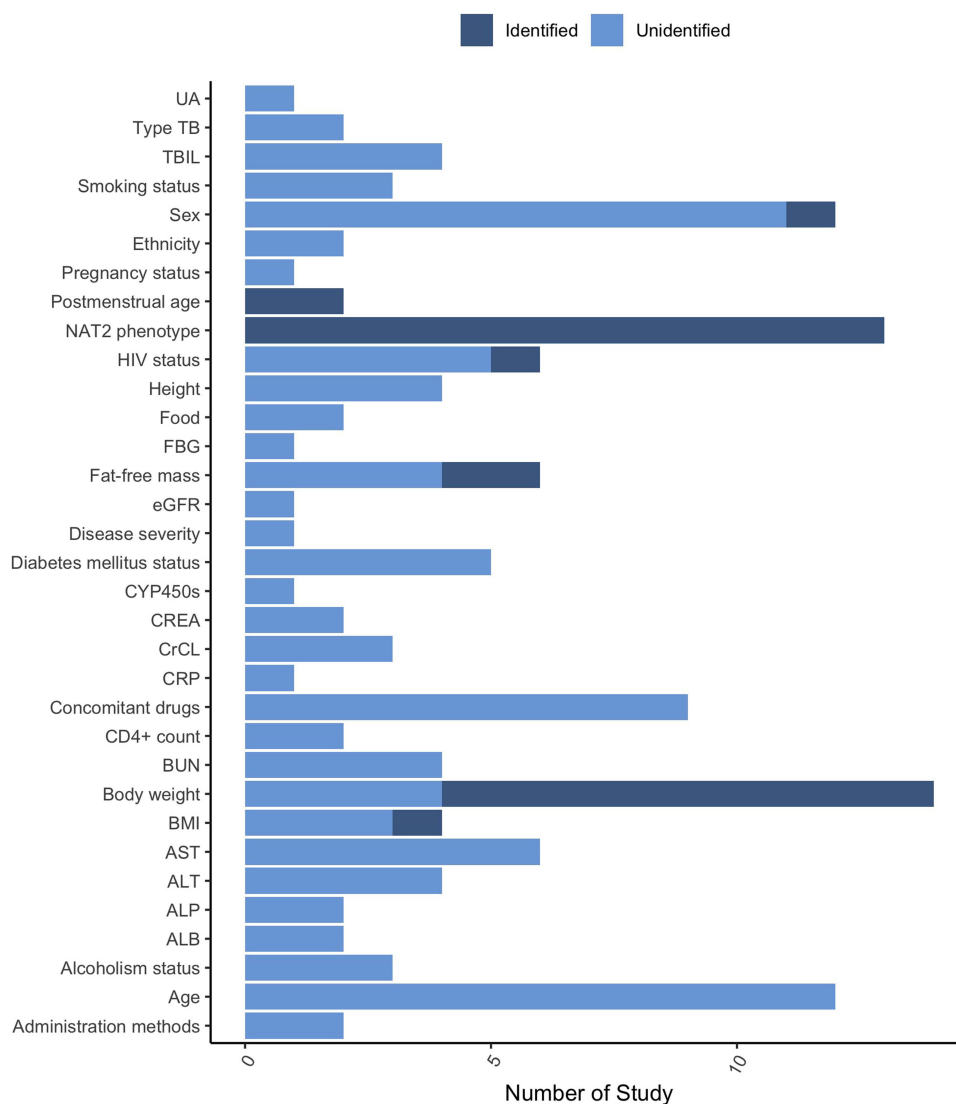


**Figure 2** Investigated and identified covariates for clearance of isoniazid.

tested and identified covariates for CL and V is presented in [Table S2](#). The identified and unidentified covariates for CL in each study are illustrated in [Figure 2](#). The NAT2 phenotype and BW/FFM were found to significantly affect isoniazid CL in all included models. In children, postmenstrual age (PMA) was found to affect CL. However, other demographic and laboratory indices had no significant effect on CL or V. PMA at which maturation of clearance is 50% complete ( $PMA_{50}$ ) ranged from 0.829 to 1.058 years.

The forest plot of covariate effects on CL ([Figure 3](#)) showed that HIV may not be a significant covariate on isoniazid clearance. Chen et al demonstrated that the NAT2 RA phenotype had a greater effect on CL in Chinese individuals compared to others.<sup>33</sup> The influence of covariates on CL investigated by other studies revealed a similar overall trend, where significant covariates on CL were PMA, BW, and NAT2 phenotypes. No other covariates were identified.

## Application of popPK Model Repository Isoniazid PK Profiles

McCallum et al did not investigate the effect of NAT2 phenotype, and thus their study was not included in the comparative analysis of the PK profiles.<sup>36</sup> [Figure 4A](#) and [B](#) shows the concentration-time profiles of isoniazid in adults and children, respectively, based on the simulated PK profiles. Since isoniazid is rapidly eliminated, there is no drug

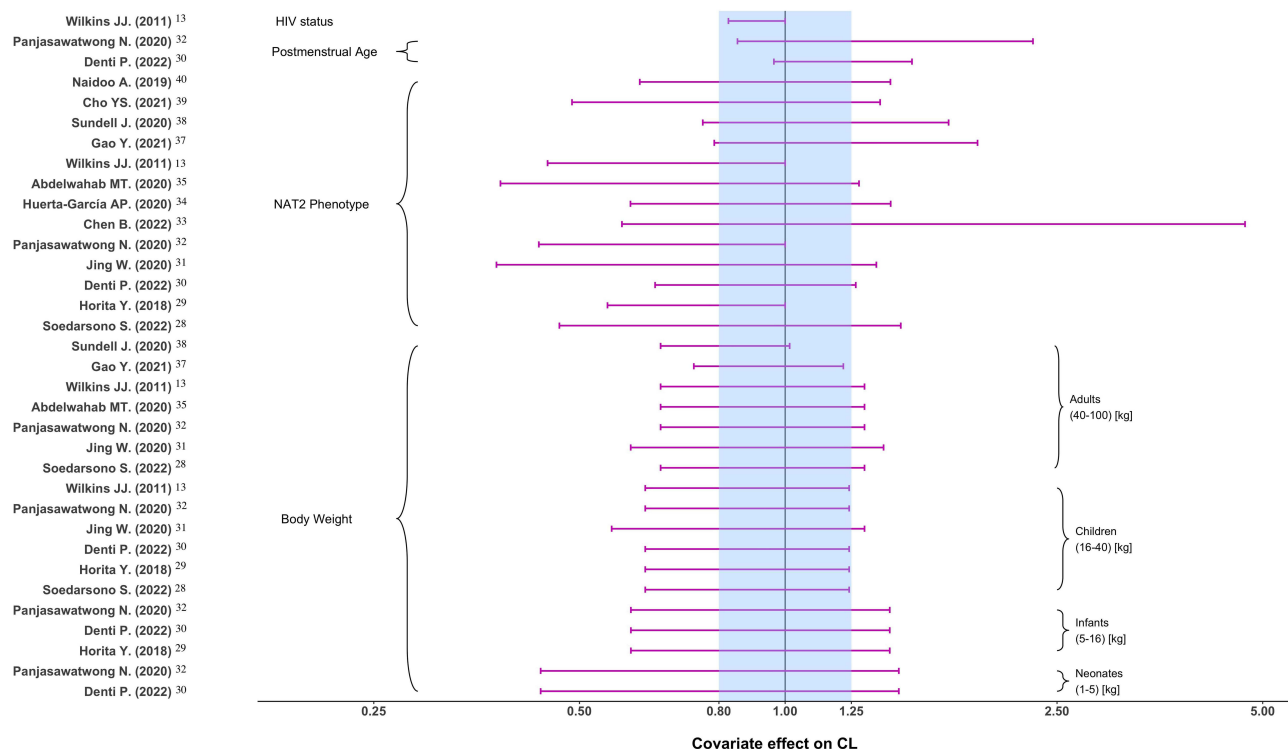


**Figure 3** Forest plot of covariates effect on the clearance of isoniazid.

**Notes:** The horizontal bars represent the covariate effect on clearance in each study. The shadow area ranges from 0.8–1.25. The study reference as below: Soedarsono S. (2022),<sup>28</sup> Horita Y. (2018),<sup>29</sup> Denti P. (2022),<sup>30</sup> Jing W. (2020),<sup>31</sup> Panjasawatwong N. (2020),<sup>32</sup> Chen B. (2022),<sup>33</sup> Huerta-García AP. (2020),<sup>34</sup> Abdelwahab MT. (2020),<sup>35</sup> Wilkins JJ. (2011),<sup>13</sup> Gao Y. (2021),<sup>37</sup> Sundell J. (2020),<sup>38</sup> Cho Y. S. (2021),<sup>39</sup> Naidoo A. (2019).<sup>40</sup>

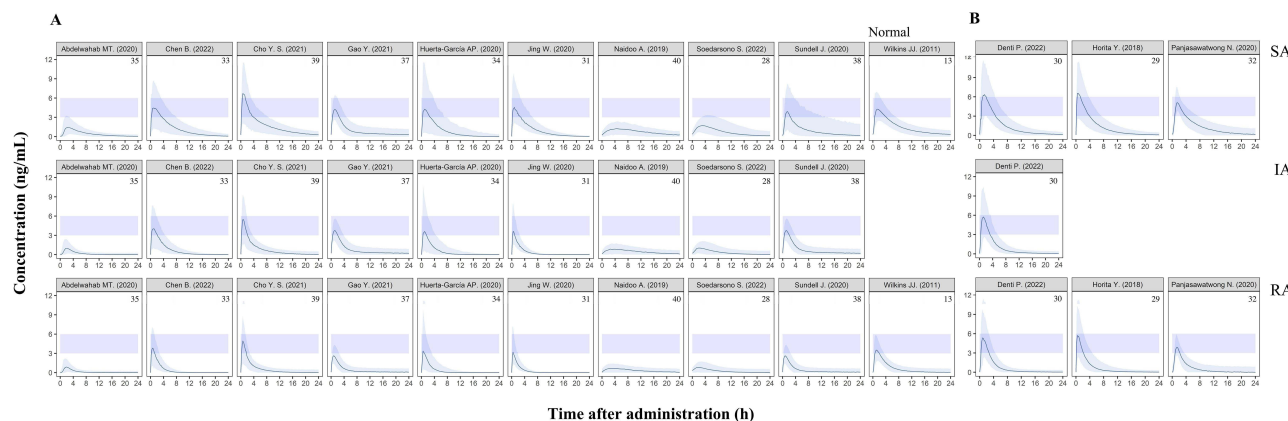


**Figure 4** Concentration-time profiles at steady state for NAT2 phenotype of SA, IA, RA or non-SA in retrieved studies.

**Notes:** (A) Adult patients; (B) Pediatric patients. The study reference as below: Soedarsono S. (2022),<sup>28</sup> Horita Y. (2018),<sup>29</sup> Denti P. (2022),<sup>30</sup> Jing W. (2020),<sup>31</sup> Panjasawatwong N. (2020),<sup>32</sup> Chen B. (2022),<sup>33</sup> Huerta-García AP. (2020),<sup>34</sup> Abdelwahab MT. (2020),<sup>35</sup> Wilkins JJ. (2011),<sup>13</sup> Gao Y. (2021),<sup>37</sup> Sundell J. (2020),<sup>38</sup> Cho Y. S. (2021),<sup>39</sup> Naidoo A. (2019).<sup>40</sup>

accumulation with standard once-daily dosing. Several studies, including those by Chen, Huerta, Jing, Wilkins, Gao, and Sundell, have reported similar exposure levels with the same dose and body weight,<sup>13,31,33,34,37,38</sup> while Abdelwahab, Soedarsono and Naidoo’s studies indicated a significant decrease in  $C_{max}$ .<sup>28,35,40</sup> The NAT2 phenotype was found to have a significant impact on isoniazid exposure, although it did not result in substantial differences in  $C_{max}$ . This article aims to establish a model repository of isoniazid and investigate significant covariates to inform clinical precision dosing.

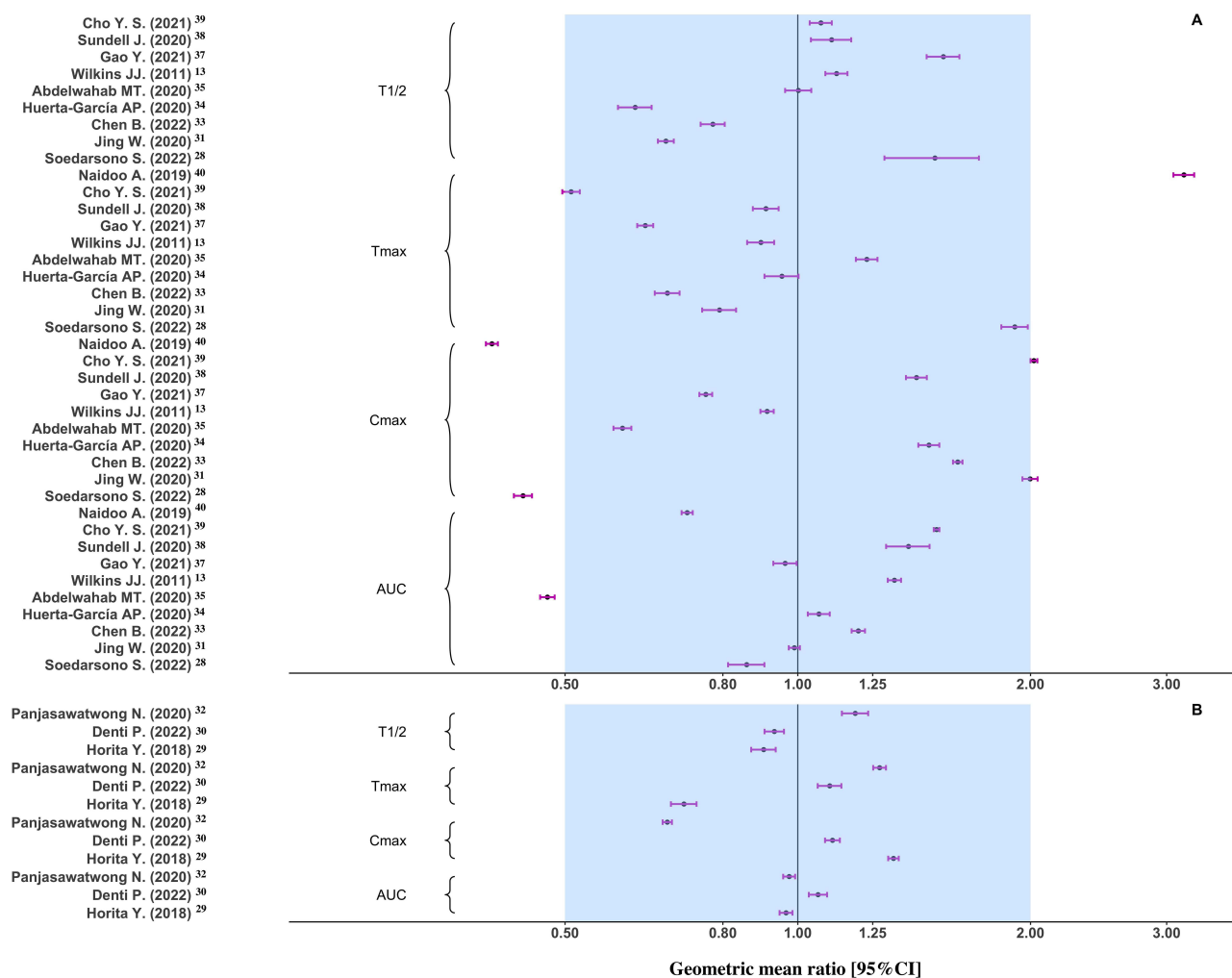


**Figure 5** Geometric mean ratio of virtual patients PK parameters in retrieved studies.

**Notes:** The horizontal bars represent the geometric mean ratio with 90% CI of NCA results (virtual patients N=1000) in retrieved studies. The shadow area ranges from 0.50–2.00; **(A)** Adult patients; **(B)** Pediatric patients. The study reference as below: Soedarsono S. (2022),<sup>28</sup> Horita Y. (2018),<sup>29</sup> Denti P. (2022),<sup>30</sup> Jing W. (2020),<sup>31</sup> Panjasawatwong N. (2020),<sup>32</sup> Chen B. (2022),<sup>33</sup> Huerta-García AP. (2020),<sup>34</sup> Abdelwahab MT. (2020),<sup>35</sup> Wilkins JJ. (2011),<sup>13</sup> Gao Y. (2021),<sup>37</sup> Sundell J. (2020),<sup>38</sup> Cho Y. S. (2021),<sup>39</sup> Naidoo A. (2019).<sup>40</sup>

## Exposure in vivo

This study presents an overview of isoniazid exposure-related parameters across various populations, graphically represented in Figure 5A and B. Most studies report geometric mean ratios of pharmacokinetic parameters within an acceptable range of 50.00%-200.00%. However, Abdelwahab's study reports lower predictions of  $AUC_{0-24}$  than the other studies,<sup>35</sup> and Soedarsono and Naidoo's study reports lower  $C_{max}$ .<sup>28,40</sup> Pregnant individuals display lower isoniazid exposure than other adult populations, whereas pediatric patients' exposure in the included studies is comparable.<sup>29,30,32</sup> The NCA of typical patients simulated in each study is summarized in Table 3, indicating that most individuals cannot achieve the expected exposure level with standard administration. Although a significant proportion of the population can achieve high  $C_{max}$ , their  $AUC_{0-24}$  levels remain below the standard required for effective treatment. Infants exhibit an earlier  $T_{max}$  and shorter  $T_{1/2}$  than adults. Moreover, a considerable decrease in the exposure of isoniazid was observed in RA or nonSA infants patients compared with SA patients, with  $AUC_{0-24}$  at 59.5% (22.63/38.01) and  $C_{max}$  at 83.2% (7.99/9.61) after standard treatment. Similarly, the exposure of nonSA (including IA, RA) adult patients significantly decreased compared with SA patients, with  $AUC_{0-24}$  at 49.3% (14.00/28.35) and  $C_{max}$  at 73.5% (4.44/6.04).

**Table 3** Non-Compartment Analysis for Virtual Patients of Involved Studies

Study (Publication Year)	Population				Dose	Tau	C <sub>max</sub> [90% CI]	AUC <sub>0-24</sub> [90% CI]	T <sub>max</sub> [90% CI]	T <sub>1/2</sub> [90% CI]
	Population	BW (kg)	PMA (years)	NAT2 phenotype						
Soedarsono S. (2022) <sup>28</sup>	Adult	60	-	SA	300	24	2.67 [2.59–2.74]	24.35 [23.04–25.67]	3.91 [3.75–4.06]	6.56 [5.79–7.33]
		60	-	IA	300	24	1.88 [1.83–1.92]	13.76 [13.28–14.23]	3.92 [3.68–4.15]	11.90 [7.58–16.22]
		60	-	RA	300	24	1.65 [1.62–1.68]	11.51 [11.19–11.82]	4.36 [4.07–4.65]	15.40 [4.39–26.41]
Horita Y. (2018) <sup>29</sup>	Infants	14	2.75	SA	150	24	12.77 [12.57–12.97]	36.71 [36.00–37.41]	0.96 [0.92–0.99]	3.51 [3.38–3.63]
		14	2.75	NonSA	150	24	11.16 [10.97–11.36]	22.82 [22.18–23.46]	0.75 [0.72–0.78]	3.67 [3.53–3.81]
Denti P. (2022) <sup>30</sup>	Infants	14	2.75	SA	150	24	10.65 [10.42–10.89]	40.38 [39.28–41.48]	1.48 [1.42–1.53]	3.62 [3.52–3.72]
		14	2.75	IA	150	24	9.60 [9.40–9.81]	27.60 [26.90–28.30]	1.30 [1.25–1.34]	3.59 [3.48–3.70]
		14	2.75	RA	150	24	8.93 [8.73–9.12]	22.49 [21.97–23.02]	1.19 [1.15–1.23]	3.56 [3.42–3.69]
Jing W. (2020) <sup>31</sup>	Adult	60	-	SA	300	24	12.06 [11.79–12.34]	28.07 [27.60–28.53]	1.62 [1.54–1.70]	2.94 [2.87–3.01]
		60	-	IA	300	24	8.38 [8.17–8.59]	10.41 [10.24–10.58]	0.88 [0.84–0.92]	1.43 [1.40–1.46]
		60	-	RA	300	24	7.29 [7.10–7.47]	7.80 [7.67–7.93]	0.80 [0.76–0.84]	1.20 [1.18–1.23]
Panjasawatwong N. (2020) <sup>32</sup>	Infants	14	2.75	SA	150	24	6.51 [6.42–6.60]	37.05 [36.39–37.71]	1.71 [1.68–1.74]	4.61 [4.43–4.79]
		14	2.75	NonSA	150	24	5.12 [5.05–5.19]	22.59 [22.32–22.86]	1.46 [1.44–1.49]	5.48 [5.16–5.79]
Chen B. (2022) <sup>33</sup>	Adult	60	-	SA	300	24	9.73 [9.59–9.86]	33.96 [33.28–34.64]	1.39 [1.34–1.44]	3.39 [3.26–3.51]
		60	-	IA	300	24	8.30 [8.17–8.42]	19.40 [19.01–19.79]	1.08 [1.04–1.12]	2.16 [2.10–2.23]
		60	-	RA	300	24	7.32 [7.21–7.43]	11.41 [11.18–11.64]	0.81 [0.78–0.84]	1.30 [1.26–1.34]
Huerta-García AP. (2020) <sup>34</sup>	Adult	60	-	SA	300	24	8.93 [8.65–9.21]	30.20 [29.21–31.18]	1.95 [1.85–2.05]	2.69 [2.55–2.82]
		60	-	IA	300	24	7.17 [6.90–7.43]	17.34 [16.75–17.93]	1.49 [1.41–1.57]	1.88 [1.80–1.97]
		60	-	RA	300	24	6.13 [5.90–6.36]	11.98 [11.55–12.41]	1.29 [1.23–1.36]	1.45 [1.38–1.52]
Abdelwahab MT. (2020) <sup>35</sup>	Pregnant Adult	60	-	SA	300	24	3.58 [3.49–3.68]	13.45 [13.16–13.74]	2.51 [2.43–2.59]	4.37 [4.20–4.54]
		60	-	IA	300	24	2.66 [2.59–2.73]	7.40 [7.29–7.50]	2.21 [2.14–2.29]	5.62 [5.27–5.96]
		60	-	RA	300	24	2.44 [2.37–2.51]	6.61 [6.52–6.70]	2.11 [2.04–2.18]	5.89 [5.38–6.41]
Wilkins JJ. (2011) <sup>13</sup>	Adult	60	-	SA	150	24	5.51 [5.40–5.62]	37.81 [37.06–38.56]	1.83 [1.76–1.91]	4.89 [4.73–5.06]
		60	-	NonSA	150	24	4.61 [4.51–4.71]	20.82 [20.50–21.14]	1.45 [1.40–1.51]	4.69 [4.49–4.89]
McCallum A. D. (2021) <sup>36</sup>	Adult	60	-	-	300	24	11.72 [11.39–12.04]	30.78 [29.69–31.87]	2.58 [2.43–2.73]	3.89 [3.69–4.08]
Gao Y. (2021) <sup>37</sup>	Adult	60	-	SA	300	24	4.59 [4.51–4.68]	27.31 [26.36–28.25]	1.30 [1.27–1.33]	6.73 [6.40–7.01]
		60	-	IA	300	24	4.14 [4.06–4.22]	23.01 [22.25–23.77]	1.20 [1.17–1.24]	7.06 [6.53–7.60]
		60	-	RA	300	24	3.06 [2.99–3.13]	15.00 [14.64–15.36]	1.07 [1.00–1.13]	9.18 [8.21–10.16]
Sundell J. (2020) <sup>38</sup>	Adult	60	-	SA	300	24	8.60 [8.34–8.87]	39.43 [36.88–41.98]	1.86 [1.79–1.93]	4.82 [4.53–5.11]
		60	-	IA	300	24	7.93 [7.69–8.17]	32.93 [30.77–35.08]	1.78 [1.73–1.84]	4.62 [4.38–4.86]
		60	-	RA	300	24	6.17 [6.03–6.32]	17.27 [16.35–18.18]	1.50 [1.46–1.54]	3.47 [3.33–3.62]
Cho Y. S. (2021) <sup>39</sup>	Adult	FFM: 46 kg	-	SA	300	24	12.20 [12.08–12.33]	42.87 [42.51–43.23]	1.04 [1.01–1.07]	4.67 [4.52–4.82]
		FFM: 46 kg	-	IA	300	24	9.52 [9.42–9.62]	23.44 [23.27–23.62]	0.84 [0.82–0.87]	4.24 [4.09–4.39]
		FFM: 46 kg	-	RA	300	24	8.51 [8.41–8.61]	18.87 [18.74–19.00]	0.77 [0.75–0.79]	4.61 [4.43–4.79]
Naidoo A. (2019) <sup>40</sup>	Adult	FFM: 46 kg	-	SA	300	24	2.43 [2.39–2.47]	20.40 [20.06–20.74]	6.46 [6.26–6.66]	11.42 [6.36–16.48]
		FFM: 46 kg	-	IA	300	24	1.81 [1.78–1.84]	14.36 [14.15–14.56]	5.85 [5.61–6.09]	10.16 [8.21–12.12]
		FFM: 46 kg	-	RA	300	24	1.52 [1.50–1.55]	11.85 [11.72–12.00]	5.97 [5.70–6.24]	Inestimable

**Abbreviations:** BW, body weight; PMA, postmenstrual age; NAT2, NAT2, N-acetyltransferase 2; SA, slow acetylators; IA, intermediate acetylators; RA, rapid acetylators; C<sub>max</sub>, peak plasma concentration (mg/L); AUC, area under the plasma concentration-time curve; T<sub>max</sub>, peak time; T<sub>1/2</sub>, half-life time; CI, confidence interval.

The isoniazid-related R codes model repository was included in the [Supplementary Material 1](#). Researchers can adjust the covariate information of the virtual population to simulate the specific model and compare the PK performance of the real-world population.

## Discussion

This study developed a model repository for isoniazid using Monte Carlo simulations to analyze the effects of covariates and generate concentration-time profiles. Our findings revealed noteworthy differences in pharmacokinetics between adults and children. Furthermore, we propose a method for MIPD in adults based on body weight and NAT2 phenotype, and an additional index based on postmenstrual age for young children. Moreover, our results show that pregnant women display lower exposure to isoniazid than other adult populations.

## Covariates Effects on Estimated PK Parameters

All 14 studies included in our analysis identified BW as a covariate on CL or V. Among these studies, 10 demonstrated that BW has a significant effect on CL, and 7 showed that BW has a significant effect on V. Our results suggest that as age increases, the impact of BW on CL or V decreases. Notably, in neonates, the effect of weight on CL was substantial, with the clearance of those at the highest BW (5 kg) being at least 1.47 times that of neonates weighing 3 kg. In contrast, the difference in CL between the heaviest adult patient (weighing 90 kg) and the lightest patient (weighing 50 kg) was at most only 1.55 times. This phenomenon is due to allometric scaling in the pediatric population, and BW is often considered a significant covariate in pediatric studies but is rarely included in adult studies.<sup>41</sup> Two studies also suggested that FFM was more suitable than BW as an allometric scaling model index.<sup>39,40</sup> It is suggested that the FFM should be included in subsequent popPK studies and compared with BW model fitting.

Thirteen of the 14 models included in our analysis identified NAT2 phenotype as a covariate on CL. Isoniazid is mainly eliminated by metabolism, with acetylation being the most important pathway. The enzyme involved in this metabolism, NAT2, is characterized by a bimodal distribution that is genetically determined.<sup>42</sup> However, there is no model to investigate the effect of NAT2 single nucleotide polymorphisms on isoniazid exposure. Six of the 14 models explored the effect of HIV status on CL, and only one study identified this covariate. Our results indicate that stratification by HIV status has no significant clinical implications for differences in isoniazid exposure in TB patients. We also suggest that subsequent popPK studies examine the NAT2 single nucleotide polymorphism variables, and other liver and kidney function indicators, HIV status, alcohol consumption, smoking, diabetes status, and drug combination may have little effect on isoniazid exposure.

## Simulations of Isoniazid

The PK profiles of isoniazid in most studies exhibit a similar curve in the typical population with standard administration, except for Abdelwahab, Soedarsono and Naidoo's studies which present different simulation profiles.<sup>28,35,40</sup> Compared with other studies, the T<sub>max</sub> of Soedarsono and Naidoo lagged significantly, which may be due to the fact that the samples of the two studies were concentrated after 2h, while the T<sub>max</sub> of other studies was mostly between 0.5–2.0h, and the absorption process of drugs in these two studies may not be accurately estimated.<sup>28,40</sup> On the other hand, Abdelwahab's study only involved pregnant women and utilized a sparse sampling strategy (SS), which only collected samples at 2, 4, 6, and 8 hours post-administration. The authors found that isoniazid exposure was significantly lower in this study than in other PK studies of isoniazid among pregnant women in South Africa.<sup>35</sup> The model repository's simulation outcomes indicate that the current SS strategy of isoniazid may be insufficient to fully capture its PK characteristics, and optimized sampling is necessary. The difference in exposure of Abdelwahab may be due to its population-dependent sampling strategy, and more exploration is needed.

After stratifying the NAT2 phenotype, the simulation results of the model repository reveal that patients with different genotypes have significant differences in exposure of isoniazid. Patients with IA and RA treated with conventional doses may fail due to inadequate exposure. The simulation results further suggest that the effects of BW and NAT2 phenotype should be considered in adult isoniazid exposure, while the effects of PMA should be considered in children.

The present study investigated the PK parameters of isoniazid in virtual patients from various populations. The results of the NCA revealed that the geometric mean ratio (90% CI) of PK parameters in most studies fell within the acceptable range of 50.00%-200.00%. However, Soedarsono's study reported  $C_{\max}$  values below the acceptable limits predicted by the model, highlighting the limitations of current sampling designs in characterizing isoniazid exposure.<sup>28</sup> Moreover, the  $T_{\max}$  of the pediatric population was found to be earlier than that of adults, indicating the need for different sampling protocols in children. Notably, an  $AUC_{0-24}$  value of 11.95 mg\*h/L was associated with treatment failure in Indian children, especially those younger than 3 years.<sup>15</sup> The observed differences in exposure between patients with RA and SA further suggest that patients with RA require a higher dose to attain the target value. These findings emphasize the need for tailored dosing strategies to achieve optimal isoniazid exposure across different patient populations.

## Uses of the Model Repository on Population PK Model Development

Our study aimed to construct a parametric popPK model repository of isoniazid for model-informed precision dosage. By utilizing our repository, researchers can rapidly simulate different clinical strategies in special patient populations, and conduct external evaluations on their own data to identify a suitable model or to investigate factors that influence predictive ability. Additionally, model selection/averaging methods can be employed to mitigate the impact of uncertainty in a single model and identify the most appropriate predictions for individual patients, thereby simplifying the precision dosing process and reducing the burden of model validation.<sup>23,24</sup> Our popPK model repository, along with other PK tools in R, can facilitate further research, such as using the PopED (<https://andrewooker.github.io/PopED/index.html>) packages to optimize clinical protocols.<sup>43</sup>

## Limitations

Our study has several limitations that should be noted. Firstly, due to the complexity and difficulty of the model, the models caused by incomplete model parameters or non-parametric method cannot be successfully reproduced, which also makes the selection of all poppk models in this study. Secondly, we selected typical populations to simulate and did not account for real-world population characteristics. Therefore, the simulation results may not be entirely representative of the covariate distribution in clinical practice. Nonetheless, these limitations offer opportunities for future research to address and refine our findings.

## Conclusion

In order to facilitate MIPD and individual medication of isoniazid, the use of a repository of parametric population pharmacokinetic models is necessary and beneficial. The optimization of isoniazid dosing regimens should take into account various factors, including the patient's BW and NAT2 phenotype in adult populations, as well as PMA in young children, among other external covariates. Our model repository presents a valuable resource for clinicians seeking to select optimal administration regimens and conduct effective therapeutic drug monitoring.

## Acknowledgments

Thanks to Changsha Duxact Clinical Laboratory Co., Ltd and Phamark Data Technology Co, Ltd, Changsha, Hunan, China for the statistical support.

## Funding

The research was funded by the Hunan graduate Research Innovation Project (grant number CX20220131), the National Natural Science Foundation of China (grant number 81803837), the Natural Science Foundation of Hunan Province (grant number 2022JJ80100, 2019JJ50839), the Hunan Province Foundation of High-level Health Talent (grant number 225), and the Science and Technology Key Program of Hunan Provincial Health Committee (grant number 20201904).

## Disclosure

The authors report no competing interests in this work.

## References

1. World Health Organization. Global tuberculosis report; 2022. Available from: <https://www.who.int/publications-detail-redirect/9789240061729>. Accessed March 8, 2024.
2. Alsultan A, Pelloquin CA. Therapeutic drug monitoring in the treatment of tuberculosis: an update. *Drugs*. 2014;74(8):839–854. doi:10.1007/s40265-014-0222-8
3. Pelloquin CA, Davies GR. The Treatment of Tuberculosis. *Clin Pharmacol Ther*. 2021;110(6):1455–1466. doi:10.1002/cpt.2261
4. World Health Organization. WHO consolidated guidelines on tuberculosis: tuberculosis preventive treatment: module 1: prevention; 2020. Available from: <https://www.who.int/publications/i/item/9789240001503>. Accessed March 8, 2024.
5. Jayaram R, Shandil RK, Gaonkar S, et al. Isoniazid pharmacokinetics-pharmacodynamics in an aerosol infection model of tuberculosis. *Antimicrob Agents Chemother*. 2004;48(8):2951–2957. doi:10.1128/AAC.48.8.2951-2957.2004
6. Gumbo T, Louie A, Liu W, et al. Isoniazid bactericidal activity and resistance emergence: integrating pharmacodynamics and pharmacogenomics to predict efficacy in different ethnic populations. *Antimicrob Agents Chemother*. 2007;51(7):2329–2336. doi:10.1128/AAC.00185-07
7. Pasipanodya JG, McIlleron H, Burger A, et al. Serum drug concentrations predictive of pulmonary tuberculosis outcomes. *J Infect Dis*. 2013;208(9):1464–1473. doi:10.1093/infdis/jit352
8. Sturkenboom MGG, Mårtson A-G, Svensson EM, et al. Population Pharmacokinetics and Bayesian Dose Adjustment to Advance TDM of Anti-TB Drugs. *Clin Pharmacokinet*. 2021;60(6):685–710. doi:10.1007/s40262-021-00997-0
9. Martson AG, Burch G, Ghimire S, et al. Therapeutic drug monitoring in patients with tuberculosis and concurrent medical problems. *Expert Opin Drug Metab Toxicol*. 2021;17(1):23–39. doi:10.1080/17425255.2021.1836158
10. Parkin DP, Vandenplas S, Botha FJ, et al. Trimodality of isoniazid elimination: phenotype and genotype in patients with tuberculosis. *Am J Respir Crit Care Med*. 1997;155(5):1717–1722. doi:10.1164/ajrccm.155.5.9154882
11. Donald PR, Parkin DP, Seifart HI, et al. The influence of dose and N-acetyltransferase-2 (NAT2) genotype and phenotype on the pharmacokinetics and pharmacodynamics of isoniazid. *Eur J Clin Pharmacol*. 2007;63(7):633–639. doi:10.1007/s00228-007-0305-5
12. Garcia-Cremades M, Solans BP, Strydom N, et al. Emerging therapeutics, technologies, and drug development strategies to address patient nonadherence and improve tuberculosis treatment. *Annu Rev Pharmacol Toxicol*. 2022;62(1):197–210. doi:10.1146/annurev-pharmtox-041921-074800
13. Wilkins JJ, Langdon G, McIlleron H, et al. Variability in the population pharmacokinetics of isoniazid in South African tuberculosis patients. *Br J Clin Pharmacol*. 2011;72(1):51–62. doi:10.1111/j.1365-2125.2011.03940.x
14. Pasipanodya JG, Srivastava S, Gumbo T. Meta-analysis of clinical studies supports the pharmacokinetic variability hypothesis for acquired drug resistance and failure of antituberculosis therapy. *Clin Infect Dis*. 2012;55(2):169–177. doi:10.1093/cid/cis353
15. Swaminathan S, Pasipanodya JG, Ramachandran G, et al. Drug concentration thresholds predictive of therapy failure and death in children with tuberculosis: bread crumb trails in random forests. *Clin Infect Dis*. 2016;63(suppl 3):S63–s74. doi:10.1093/cid/ciw471
16. Erwin ER, Addison AP, John SF, et al. Pharmacokinetics of isoniazid: the good, the bad, and the alternatives. *Tuberculosis*. 2019;116:S66–s70. doi:10.1016/j.tube.2019.04.012
17. Torok ME, Aljayoussi G, Waterhouse D, et al. Suboptimal exposure to anti-TB drugs in a TBM/HIV+ Population is not related to antiretroviral therapy. *Clin Pharmacol Ther*. 2018;103(3):449–457. doi:10.1002/cpt.646
18. Darwich AS, Polasek TM, Aronson JK, et al. Model-informed precision dosing: background, requirements, validation, implementation, and forward trajectory of individualizing drug therapy. *Annu Rev Pharmacol Toxicol*. 2021;61(1):225–245. doi:10.1146/annurev-pharmtox-033020-113257
19. Qin Y, Zhang -L-L, Ye Y-R, et al. Parametric population pharmacokinetics of linezolid: a systematic review. *Br J Clin Pharmacol*. 2022;88(9):4043–4066. doi:10.1111/bcp.15368
20. Chen YT, Wang C-Y, Yin Y-W, et al. Population pharmacokinetics of oxcarbazepine: a systematic review. *Expert Rev Clin Pharmacol*. 2021;14(7):853–864. doi:10.1080/17512433.2021.1917377
21. Li ZR, Wang C-Y, Zhu X, et al. Population Pharmacokinetics of Levetiracetam: a Systematic Review. *Clin Pharmacokinet*. 2021;60(3):305–318. doi:10.1007/s40262-020-00963-2
22. Liu X, Ju G, Yang W, et al. Escitalopram personalized dosing: a population pharmacokinetics repository method. *Drug Des Devel Ther*. 2023;17:2955–2967. doi:10.2147/DDDT.S425654
23. Uster DW, Stocker SL, Carland JE, et al. A model averaging/selection approach improves the predictive performance of model-informed precision dosing: vancomycin as a case study. *Clin Pharmacol Ther*. 2021;109(1):175–183. doi:10.1002/cpt.2065
24. Kantasiripitak W, Outtier A, Wicha SG, et al. Multi-model averaging improves the performance of model-guided infliximab dosing in patients with inflammatory bowel diseases. *CPT Pharmacometrics Syst Pharmacol*. 2022;11(8):1045–1059. doi:10.1002/psp4.12813
25. Tan WR, Noor Harun &, Sheikh Ghadzi &M, et al. Systematic review of population pharmacokinetic models of isoniazid in children and adults with tuberculosis. *Malaysian J Pharm*. 2022;8(2):1–15. doi:10.52494/DJIQ7058
26. Thomas L, Raju AP. Influence of N-acetyltransferase 2 (NAT2) genotype/single nucleotide polymorphisms on clearance of isoniazid in tuberculosis patients: a systematic review of population pharmacokinetic models. *Eur J Clin Pharmacol*. 2022;78(10):1535–1553. doi:10.1007/s00228-022-03362-7
27. Li J, Cai X, Chen Y, et al. Parametric population pharmacokinetics of isoniazid: a systematic review. *Expert Rev Clin Pharmacol*. 2023;16(5):467–489. doi:10.1080/17512433.2023.2196401
28. Soedarsono S, Jayanti RP, Mertaniasih NM, et al. Development of population pharmacokinetics model of isoniazid in Indonesian patients with tuberculosis. *Int J Infect Dis*. 2022;117:8–14. doi:10.1016/j.ijid.2022.01.003
29. Horita Y, Alsultan A, Kwara A, et al. Evaluation of the adequacy of WHO revised dosages of the first-line antituberculosis drugs in children with tuberculosis using population pharmacokinetic modeling and simulations. *Antimicrob Agents Chemother*. 2018;62(9). doi:10.1128/AAC.00008-18
30. Denti P, Wasmann RE, van Rie A, et al. Optimizing dosing and fixed-dose combinations of rifampicin, isoniazid, and pyrazinamide in pediatric patients with tuberculosis: a prospective population pharmacokinetic study. *Clin Infect Dis*. 2022;75(1):141–151. doi:10.1093/cid/ciab908
31. Jing W, Zong Z, Tang B, et al. Population pharmacokinetic analysis of isoniazid among pulmonary tuberculosis patients from China. *Antimicrob Agents Chemother*. 2020;64(3). doi:10.1128/AAC.01736-19

32. Panjasawatwong N, Wattanakul T, Hoglund RM, et al. Population pharmacokinetic properties of antituberculosis drugs in Vietnamese children with tuberculous meningitis. *Antimicrob Agents Chemother.* 2020;65(1). doi:10.1128/AAC.00487-20
33. Chen B, Shi H-Q, Feng MR, et al. Population pharmacokinetics and pharmacodynamics of isoniazid and its metabolite acetylisoniazid in Chinese population. *Front Pharmacol.* 2022;13:932686. doi:10.3389/fphar.2022.932686
34. Huerta-Garcia AP, Medellin-Garibay SE, Ortiz-álvarez A, et al. Population pharmacokinetics of isoniazid and dose recommendations in Mexican patients with tuberculosis. *Int J Clin Pharm.* 2020;42(4):1217–1226. doi:10.1007/s11096-020-01086-1
35. Abdelwahab MT, Leisegang R, Dooley KE, et al. Population pharmacokinetics of isoniazid, pyrazinamide, and ethambutol in pregnant South African Women with tuberculosis and HIV. *Antimicrob Agents Chemother.* 2020;64(3). doi:10.1128/AAC.01978-19
36. McCallum AD, Pertinez HE, Else LJ, et al. Intrapulmonary pharmacokinetics of first-line anti-tuberculosis drugs in Malawian patients with tuberculosis. *Clin Infect Dis.* 2021;73(9):e3365–e3373. doi:10.1093/cid/ciaa1265
37. Gao Y, Davies Forsman L, Ren W, et al. Drug exposure of first-line anti-tuberculosis drugs in China: a prospective pharmacological cohort study. *Br J Clin Pharmacol.* 2021;87(3):1347–1358. doi:10.1111/bcp.14522
38. Sundell J, Bienvenu E, Janzén D, et al. Model-based assessment of variability in isoniazid pharmacokinetics and metabolism in patients co-infected with tuberculosis and HIV: implications for a Novel Dosing Strategy. *Clin Pharmacol Ther.* 2020;108(1):73–80. doi:10.1002/cpt.1806
39. Cho YS, Jang TW, Kim H-J, et al. Isoniazid population pharmacokinetics and dose recommendation for Korean patients with tuberculosis based on target attainment analysis. *J Clin Pharmacol.* 2021;61(12):1567–1578. doi:10.1002/jcph.1931
40. Naidoo A, Chirehwa M, Ramsuran V, et al. Effects of genetic variability on rifampicin and isoniazid pharmacokinetics in South African patients with recurrent tuberculosis. *Pharmacogenomics.* 2019;20(4):225–240. doi:10.2217/pgs-2018-0166
41. Mahmood I. Misconceptions and issues regarding allometric scaling during the drug development process. *Expert Opin Drug Metab Toxicol.* 2018;14(8):843–854. doi:10.1080/17425255.2018.1499725
42. Rey E, Gendrel D, Treluyer JM, et al. Isoniazid pharmacokinetics in children according to acetylator phenotype. *Fundam Clin Pharmacol.* 2001;15(5):355–359. doi:10.1046/j.1472-8206.2001.00044.x
43. Foracchia M, Hooker A, Vicini P, et al. POPED, a software for optimal experiment design in population kinetics. *Comput Methods Programs Biomed.* 2004;74(1):29–46. doi:10.1016/S0169-2607(03)00073-7

## Drug Design, Development and Therapy

Dovepress

### Publish your work in this journal

Drug Design, Development and Therapy is an international, peer-reviewed open-access journal that spans the spectrum of drug design and development through to clinical applications. Clinical outcomes, patient safety, and programs for the development and effective, safe, and sustained use of medicines are a feature of the journal, which has also been accepted for indexing on PubMed Central. The manuscript management system is completely online and includes a very quick and fair peer-review system, which is all easy to use. Visit <http://www.dovepress.com/testimonials.php> to read real quotes from published authors.

Submit your manuscript here: <https://www.dovepress.com/drug-design-development-and-therapy-journal>